UCID- 20569, Rev. 1

THE IMPACT OF SEVERAL REACTOR FEATURES ON TF COIL DESIGN FOR TPSS

J. R. Miller and R. H. Bulmer

CIRCULATION COPY
SUBJECT TO RECALL
IN TWO WEEKS

March 26, 1986

This is an informal report intended primarily for internal or limited external distribution. The opinions and conclusions stated are those of the author and may or may not be those of the Laboratory.
Work performed under the auspices of the U.S. Department of Energy by the Lawrence Livermore National Laboratory under Contract W-7405-Eng-48.

Lawrence Livermore National Laboratory

DISCLAIMER

This document was prepared as an account of work sponsored by an agency of the United States Government. Neither the United States Government nor the University of California nor any of their employees, makes any warranty, express or implied, or assumes any legal liability or responsibility for the accuracy, completeness, or usefulness of any information, apparatus, product, or process disclosed, or represents that its use would not infringe privately owned rights. Reference herein to any specific commercial products, process, or service by trade name, trademark, manufacturer, or otherwise, does not necessarily constitute or imply its endorsement, recommendation, or favoring by the United States Government or the University of California. The views and opinions of authors expressed herein do not necessarily state or reflect those of the United States Government or the University of California, and shall not be used for advertising or product endorsement purposes.

Printed in the United States of America
Available from
National Technical Information Service
U.S. Department of Commerce
5285 Port Royal Road
Springfield, VA 22161

Price Code	Page Range
A01	Microfiche
Papercopy Prices	
A02	001-050
A03	051-100
A04	101-200
A05	201-300
A06	301-400
A07	401-500
A08	501-600
A09	601

THE IMPACT OF SEVERAL REACTOR FEATURES ON TF COIL DESIGN FOR TPSS

INTRODUCTION

Past studies that have tried to project the appearance of future fusion reactors have produced designs that were unattractive because of their high capital cost, which was due mainly to their large size. In current studies, much effort is being expended to find ways to minimize machine size and complexity in the hope that the final designs will prove less expensive. A significant driver of machine size in previous designs was the amount of nuclear shielding placed between the blanket and the toroidal field (TF) coils to minimize the radiation heating and damage in these critical components. Of course the total amount of shielding is not arbitrary; it certainly must adequately suppress radiation outside the plant. However, if all of this shielding were contained inside the TF coils, several parameters (coil size and weight, maximum field at the windings, stored energy, etc.) would become inordinately large.

Reducing the amount of shielding inside the TF coils and allowing the radiation load to climb to less "conventional" levels could pay big benefits in reducing the machine size, so long as the damage and heat load remain tolerable. Recent studies[1,2] indicate that superconducting windings in TF coils can accept much higher heat loads than have been previously considered and simultaneously can be designed with higher than conventional current densities. The purpose of the present exercise is to probe the limits of acceptable radiation levels in relation to winding pack current densities in the TF coils for reactor relevant designs.

BASELINE RADIATION LOAD

A very aggressive level of radiation will be examined in this exercise. In essence, we pose the following question: "Suppose an insulating material can be found that will survive 10^{12} rads absorbed over the life of the machine, which is assumed to be 40 full power years (fpy); can the other consequences of this level of radiation, namely 7 $mW \cdot cm^{-3}$ peak heat load in the winding pack, 4×10^{20} $n \cdot cm^{-2}$ fast neutron fluence, and 0.2 dpa damage to the copper stabilizer of the conductor, be tolerated?" Some immediate consequences of this scenario can be noted. Figure 1 gives part of the evidence suggesting that the none of the A15 compound superconductors will survive neutron fluences greater than $\sim 10^{18}$ $n \cdot cm^{-2}$. NbTi conductors probably will be useable at these levels; however, we shall see that this presents a non-trivial problem for heat removal because of the much lower critical temperature T_c of this alloy compared to the A15 compounds. The result is lower attainable maximum fields.

Force cooled conductors will be stipulated in this study because active cooling will be needed to handle the high peak heat loads, and

because cable-in-conduit, force-cooled conductors are expected to suffer much less degradation of stability due to radiation damage to the copper stabilizer. But in this type conductor, some temperature margin between inlet helium temperature and the current sharing temperature of the superconductor must be used in removing the heat and some must be maintained to stabilize the conductor against perturbations that may be imposed during operation of the magnet. It will be shown that maximum field of around 6 T, with quite reasonable winding pack current density, can be supported while maintaining adequate stability and the ability to protect the coils in the event of a quench to end of the machine life.

BASELINE TF CONFIGURATION

Several machine configurations of interest for the TPSS were suggested by D. A. Ehst.[3] The version having approximately 6 T field at the coil case (6.21 T at the windings) is characterised by the parameters listed in Table 1. More detail must be added to this list subject to various constraints and performance characteristics.

The number of coils in the TF set affects field ripple at the outer plasma edge, machine access, ease of assembly and disassembly, and (to some extent) protection. To illustrate the effect of the number of coils on field ripple, a winding pack current density J_{pack} = 60 $A \cdot mm^{-2}$ and a winding build of 0.2 m was assumed, and the calculations in Fig. 2 were performed. For 16 coils with the assumed winding geometry, the ripple is 4.4 % peak-to-peak.

The number of coils has the strongest influence, but spreading the windings might be expected to reduce the ripple somewhat. To get a feel for the magnitude of this effect, an additional 16 coil example was calculated. In this case, the same 0.2 m winding build was used, but J_{pack} was reduced to 40 $A \cdot mm^{-2}$ and the winding spread laterally to compensate. Figure 3 shows a comparison of the assumed winding shapes and lists the corresponding field ripple values. From Fig. 2 it is apparent that if field ripple no higher than 2 - 3 % can be tolerated, there may be no fewer than 18 coils, unless other means suppression techniques are used (e.g. shimming with appropriately placed ferromagnetic inserts).

WINDING PACK DESIGN

Particular features of the winding pack are often a matter of designer's choice. A successful design results when the strong features of a particular type of design are emphasized and the weak features compensated. We begin this design with a cable-in-conduit conductor (CICC). The sheath provides strong containment of the helium coolant and also adds structure at the source of the electromagnetic forces. There are benefits for maximizing the overall current density of a winding pack based on this type of conductor if

the sheath is used effectively in these roles. If it is not used effectively, it becomes a penalty to the obtainable pack current denstiy.

The CICC also allows for solid insulation between turns of conductor and thus the opportunity for higher allowable turn-to-turn and terminal voltages. It is not possible to fully optimize the fractions of steel and insulation in the winding pack without detailed knowledge of the mechanical loads, internal pressures, fault conditions, etc., but experience from previous designs where manufacturability, tensile load sharing, and support of centering loads by the conductor sheath were primary considerations suggests that 20 - 25 % of the winding pack should consist of steel and 15 - 20 % insulation. We choose f'_{steel} = 22 % and $f'_{insulation}$ = 15 % for this study. The remaining 63 %, consisting of helium, superconductor, and copper stabilizer (aluminum has been shown to be inferior in a high radiation environment[4]), must be tailored to the requirements of heat removal, protection, and stability.

Heat removal--Heat is removed in a CICC by introducing single phase He at some temperature T_{in} and forcing it through the conductor at a sufficient flow rate that the maximum temperature in the flowpath does not compromise the stability required. Of course the flow cannot be increased without limit because frictional losses become significant, and any further increase in flow gives an increase in the maximum temperature in the flowpath.[1,5] The alternative is shorter, more numerous flowpaths with the consequence of more complex manifolding for injection and removal of the helium. Good advantage can be taken of the high heat capacity of helium in the pressure range just above the critical pressure, e.g. in the range from about 300 - 500 kPa, both for steady heat removal and for stabilization.[1] Shorter channels that allow for sufficient flow, but with low enough pressure drop to stay in this range over an entire flowpath, are an attractive design option.

To test our ability to adequately remove the heat, some assumptions must be made about the distribution of heat in the windings. First, even with shielding of uniform thickness between the plasma and the circumference of the TF coils, the circumferential distribution of heat will not be uniform. This is because the outboard legs of the TF coils represent only a fraction of the total cross section intercepting the radiation of the outer plasma surface and because they are further from the plasma than are the inboard legs. The combination of effects should reduce the radiation heat load at the midplane of an outboard TF coil leg by 1/10 when compared to the maximum at the midplane of the inboard leg. Second, calculations with "typical" materials of a winding pack suggest that heating rates should fall off exponentially with depth into the pack with a characteristic (e-folding) depth of 9 - 10 cm.[4] These assumptions can be combined in the following simple form for an

approximate distribution of heating in a TF coil that will be useful for estimating purposes:

$$\dot{q}_n(r,\theta) = \dot{q}_{max} \exp[-(r - R)/0.095]\{ \sin(\theta/2) + (1/10)[1 - \sin(\theta/2)]\}$$

where R is the equivalent inner radius of a "dee" coil topologically deformed into a circle, and the angle θ is measured from a radius through the midplane of the outer leg.

From this distribution, we estimate that the average heat load into a turn of conductor in the innermost layer is

$$\langle \dot{q}_n \rangle = 0.67\ \dot{q}_{max} \approx 4.7\ kW/m^3 \quad .$$

Later, when a determination of the useable winding pack current density has been made, and the winding pack dimensions have been set, we can use the same distribution function to obtain an approximation of the total radiation heat load per coil. However, of more immediate interest is whether the average heat load per turn on the inner layer of the winding can be accomodated. Using the approximate techniques of ref. 1, it can be shown that this load can be absorbed with a temperature rise of < 0.4 K in that turn by appropriate manifolding to provide the required He flow. The conductor must be rather "open", however, and a minimum void fraction of 40 % in the cable space of the CICC is suggested to preclude too much pressure loss.

Stability--At a particular current density and field, the stability margin provided by a CICC can be expressed in the form

$$\Delta H = S_{He} \frac{f_{He}}{f_{cond}} (T_{cs} - T_b)$$

where S_{He} is the effective volumetric heat capacity of the helium between the initial bulk fluid temperature T_b and the current sharing temperature T_{cs} of the superconductor. The ratio of the helium fraction f_{He} to conductor fraction f_{cond} in the cable space merely refers the sudden absorbed energy that will just quench the conductor to a unit volume of conductor. The above relation is essentially a statement of experimental observation that, to first order, the stability of a CICC is derived from the heat capacity of the interstitial helium over the temperature range that the conductor is superconducting.[7]

The temperature dependence of the critical current density of a superconductor at the operating field is sufficiently linear over the range of interest that it can be fully represented for our purposes by the intercepts $J_{co}(B)$ and $T_c(B)$. The above can then be cast in the dimensionless form,

$$\Delta h = \frac{\Delta H}{s_{He}\, T_c} = \frac{(1 - f_{cond})}{f_{cond}} \left[\frac{(T_c - T_b)}{T_c} - \frac{J}{f_{cond}\,(1 - f_{Cu})\, J_{c0}} \right] ,$$

where J is the current density inside the cable space of the CICC and f_{cu} is the fraction of copper in the conductor strands (note that $J_{pack} = 0.63\ J$ for the fractions of steel and insulation assumed). In this form, the dimensionless stability parameter Δh has the properties of the coolant factored out, leaving only those parameters describing the conductor and the operating conditions.

Note that the above relation does not contain the resistivity of the copper stabilizer since, to first order at least, the stability margin is observed to be independent of it.[9] Rather, at a given current density, the conductor design offering the maximum stability is established by a trade off between adding more superconductor and adding more helium. The amount of superconductor of course depends on the amount of copper contained in the conductor strands (for reasons other than direct stabilization). The optimum trade off thus depends on this fraction of copper, as can be seen by examining contours of Δh in the (f_{cond}, f_{cu}) plane. A typical mapping is shown in Fig. 4 with the locus of optimum f_{cond} for fixed f_{cu}. There are of course limits to the amount of copper that can be used.

Minimum copper fraction--The processing of NbTi into practical superconducting wire requires a minimum amount of copper to be co-drawn with it. The limit is not absolute, but very few manufacturers regularly make good wire with less than 50 % copper. We will take this number as a minimum for this study, recognizing that other considerations will probably call for higher fractions anyway.

Effect of damage to copper stabilizer--The proposed level of radiation will cause an increase in the residual resistivity of the copper matrix according to a relation of the following form:

$$\Delta\rho_0 = s[1 - \exp(-iD/s)] ,$$

where s is the saturation level and i is the saturation rate. Sawan[9] gives $s = 3\ n\Omega\cdot m$ and $i = 720\ n\Omega\cdot m\cdot dpa^{-1}$ while Klabunde, et al.[4] give $s = 4\ n\Omega\cdot m$ and $i = 649\ n\Omega\cdot m\cdot dpa^{-1}$. We use $s = 3.46\ n\Omega\cdot m$ and $i = 696\ n\Omega\cdot m\cdot dpa^{-1}$ as a compromise. Magnetoresistivity is accounted for by the relation[10]

$$\rho(B) = \rho_o[1 + 0.0339(B/\rho_o)^{1.07}]$$

where ρ_o includes the effects of radiation damage.

Limiting current--The limiting current density in a CICC is the value below which full stability is available even with initially stagnant helium inside,[11] and as such may be viewed as a good indicator that heat transfer from the cable to the helium is good, even without being augmented by net flow. Therefore, choosing a conductor configuration for which the limiting current density J_{lim} exceeds the design value for the cable space current density J amounts to choosing a design that is not limited by heat transfer. Towards the end-of-life, as copper damage accumulates to reduce J_{lim}, the loss will be offset by the helium flow already required for heat removal. In Fig. 5, contours of the stability parameter have been overlaid with contours of $J_{lim} = J$ for both initial and end-of-life stabilizer resistivities. In the present study, we will observe the constraints on conductor configuration (i.e. f_{cond} and f_{Cu}) due to the former and ignore those due to the latter.

Protection--There are two major consequences that must be considered when providing for the protection of a CICC coil in the event of a quench: maintaining a safe maximum pressure inside the conduit and maintaining a safe maximum hot spot temperature of the conductor. An experimentally based, worst-case prediction shows that the former depends strongly on distance between flow connections.[12] To facilitate removal of the radiation heat loads, that distance will necessarily be short, and high quench pressure should not be a severe problem. Maximum hot spot temperature during a quench is more crucial and will in fact be the dominant limitation on the winding pack current density for the present case.

The upper limit to the cable space current density in terms of the allowed maximum hot-spot temperature can be determined from the following expression:

$$J_{prot} \le \sqrt{(2/\tau)} \left[(1 - f_{cond})\, f_{cond} f_{Cu} \int_{T_b}^{T_{max}} \frac{\mu_{He,init}\, c_{v,He}}{\rho_{Cu}}\, dT \right.$$

$$+ f_{Cu}^2 f_{cond}^2 \int_{T_b}^{T_{max}} \frac{\mu_{Cu}\, c_{Cu}}{\rho_{Cu}}\, dT$$

$$\left. + (1 - f_{Cu})\, f_{Cu}^2 f_{cond} \int_{T_b}^{T_{max}} \frac{\mu_{s.c.}\, c_{s.c.}}{\rho_{Cu}}\, dT \right]^{1/2},$$

where μ_i and c_i are the density and heat capacity, respectively, of a particular component (helium, copper, or NbTi) of the CICC and ρ_{Cu} is the electrical resistivity of the copper in the conductor. The dump time constant τ is given simply by

$$\tau = 2\, E_s / V_d\, I_{op}$$

where E_s is the stored energy per TF coil, V_d is the dump voltage across the terminals of an individual coil, and I_{op} is the operating current. Experiments simulating a fully quenched CICC[12] have shown that the initial density of the helium and the constant volume heat capacity of the helium (essentially constant and approximately equal to 3.1 $kJ \cdot kg^{-1} \cdot K^{-1}$) are the appropriate choices for the values in the first term of the above equation (as indicated).

We are free now to make several choices that are important to our estimation of the protection limit to J. The values we choose for T_{max}, V_d, and I_{op} reflect our personal assessments of the current state-of-the-art and future trends in the technologies impacted by these choices. Selecting $T_{max} \approx 100$ K ensures that differential thermal expansion of the coil components in the event of a quench will be negligible. A maximum coil terminal voltage $V_d \approx 5$ kV should be accomodated easily by a CICC design that provides solid insulation devoid of helium between conductor turns. And coil current $I_{op} \approx 30$ kA will ease the protection problem without penalizing the design with a too high refrigeration load (in comparison to that from the radiation heating) or an intractably large and difficult-to-wind conductor (especially if the operating current density can be kept high). These choices are all conservative in that they can all be pushed higher by innovative development (translate--research dollars), but first let us examine the consequences of these choices.

In Fig. 6, the contours of $J = J_{prot}$ are overlayed on contours of the stability parameter and the other limits already discussed. The lower corresponds to undamaged copper (i.e. RRR = 100 and magnetoresistance appropriate to the operating field), the next corresponds to copper damage of 0.005 dpa (1 fpy operation), and the highest to 0.2 dpa (40 fpy). With the design philosophy of selecting the conductor configuration giving the maximum stability consistent with all other limits and constraints, the conductor design proceeds as follows: Select a trial value of J and produce a mapping of the stability parameter such as that in Fig. 6. Move from the upper right to the lower left along the locus of optimum f_{cond} (increasing stability) until the contour defining some constraint is met. Move down along this constraint contour so long as stability continues to increase or until another constraint is met. Then move down along the next contour. Eventually, either a maximum available stability or the minimum copper fraction will be reached. If the resulting stability margin is higher than needed, a higher value of J can be chosen and

the selection process repeated.

This selection process is easy to automate and Figs. 7, 8, and 9 show the results of varying the cable space current density J and extracting the corresponding values of f_{cu}, f_{cond}, and Δh. The resultant copper fraction remains acceptable over the entire range examined. However, each trajectory eventually exceeds the maximum allowed conductor fraction (remember, we had decided to maintain 40 % void to alleviate heat removal). And a minimum acceptable stability parameter has also been passed (we have somewhat arbitrarily chosen h = 0.066 corresponding to a stability margin of 300 $mJ \cdot cm^{-3}$ of conductor).

As might be expected, the trajectory in each case corresponding to the highest copper damage gives the lowest allowable current density. The lowest limit to cable space current density by this design methodology is J = 59 $A \cdot mm^{-2}$ (J_{pack} = 37 $A \cdot mm^{-2}$) corresponding to the intersection of the limit on f_{cond} and the trajectory for a copper damage of 0.2 dpa. It can be seen by inspection that the portion of the trajectory at the intersection corresponds to points on the boundary for J = J_{prot}. The same is true for the trajectory for copper damage of 0.005 dpa (but not for the undamaged copper trajectory). Thus we see that for the levels of radiation being examined in this study, the winding pack current density is simultaneously being limited by considerations of heat removal and protection. Stability and minimum copper fraction are not primary constraints.

SUMMARY AND CONCLUSIONS

Table 2 lists the important TF coil and conductor characteristics obtained from this study. The following general conclusions can be made:

The fast neutron fluence of 4 x 10^{20} $n \cdot cm^{-2}$ precludes the use of Nb_3Sn and other A15 superconductors, and may preclude the consideration of fields much higher than 6 T.

At the "6 T" level considered here, accepting 7 $mW \cdot cm^{-3}$ radiation heating appears workable even with NbTi.

A decision to anneal out the copper damage at 1 fpy intervals should allow the pack current density to be about 15 % higher.

The minimum number of coils based on acceptable field ripple appears to be 18 unless alternate ripple reduction techniques are found.

Even with 18 coils, the stored energy per coil, together with the anticipated radiation damage to the copper, makes coil protection

a critical issue in setting the winding pack current density.

Table 1. Machine parameters critical to TF coil design

Physical description

Major radius	5.25 m
Field on axis	3.83 T
Mean rad., outboard	8.10 m
Mean rad., inboard	3.10 m
half height	3.22 m
Total stored energy	4.91 GJ

Nuclear environment

Nuclear heating	7 $mW \cdot cm^{-3}$
Fast neutron fluence	4×10^{20} $n \cdot cm^{-2}$
Cu damage	0.2 dpa
Insulator dose	10^{12} rads
(over 40 yrs. availability)	

Table 2. TF coil and conductor summary

TF coil characteristics

B_{max}	6.21 T
T_{inlet}	4.5 K
T_{outlet}	4.9 K
E_m	273 MJ/coil
V_d	5 kV/coil
I_{op}	30 kA
$T_{max,quench}$	100 K
J_{pack}	37 A·mm^{-2} (0.2 dpa)
	43 A·mm^{-2} (0.005 dpa)

Conductor characteristics

Type	Cu:NbTi, cable-in-conduit conductor (CICC)
f'_{insul}	0.15
f'_{steel}	0.22
f'_{cond}	0.38
f'_{He}	0.25
J_{eo}	5200 A·mm^{-2} at 6.21 T
T_c	6.53 K at 6.21 T
d_w	0.7 mm
I/I_c	0.31 (0.2 dpa)
	0.33 (0.005 dpa)

REFERENCES

1. J.R. Miller, "Design of Aggressive Superconducting TFCX Magnet Systems," presented at the 6th Topical Meeting on the Technology of Fusion Energy, San Francisco, California, March 3-7, 1985.

2. C.D. Henning, B.G. Logan, W.L. Barr, R.H. Bulmer, J.N. Doggett, B.M. Johnston, J.D. Lee, R.W. Hoard, D.S. Slack, and J.R. Miller, "A Tokamak Ignition/Burn Experimental Research Device," presented at the 6th Topical Meeting on the Technology of Fusion Energy, San Francisco, California, March 3-7, 1985.

3. D.A. Ehst, ANL, private communication, June 1985.

4. C.E. Klabunde, R.R. Coltman, Jr., and J.M. Williams, "The Effects of Irradiation on the Normal Metal of a Composite Superconductor: Copper and Aluminum," Journal of Nuclear Materials 85 & 86 (1979) 385.

5. P.A. Materna, "Design Considerations for Forced-Flow Superconductors in Toroidal Field Coils," in Proceedings of 10th Symposium on Fusion Energy, Philadelphia, Pennsylvania, December 5-9, 1983, IEEE Cat. No. 83CM1916-6, p. 1741.

6. J.D. Lee, LLNL, private communication, June 1984.

7. J.R. Miller and J.W. Lue, "Designing Internally Cooled Superconductors for Use in Large Magnets," Stability of Superconductors in HeI and HeII, Proceedings of the Workshop held at Saclay (France), International Institute of Refrigeration, Paris, France, 1981, p. 247.

8. J.R. Miller, "Empirical Investigation of Factors Affecting the Stability of Cable-In-Conduit Superconductors," Cryogenics 25 (1985) 552.

9. M.E. Sawan, "Review of Radiation Effects in Superconducting Magnets and Proposed Radiation Limits," presented at the Workshop on Radiation Limits to Superconducting Magnets, Fusion Technology Institute, University of Wisconsin, Madison Wisconsin, May 1985.

10. M.W. Guinan, "Radiation Effects Limits on Copper in Superconducting Magnets," UCID-19800, Lawrence Livermore National Laboratory, May 25, 1983.

11. L. Dresner, "Parametric Study of the Stability Margin of Cable-in-Conduit Superconductors: Theory," IEEE Trans. Magn. MAG 17 (1981) 753.

12. J.R. Miller, J.W. Lue, L. Dresner, S.S. Shen, and H.T. Yeh,

"Pressure Rise during the Quench of a Superconducting Magnet using Internally Cooled Conductors," in Proc. 8th Intern. Cryogenic Engineering Conference, IPC Science and Technology Press, Ltd., Guilford, Surrey, UK, 1980, p. 321.

FIGURE CAPTIONS

Figure 1. Effects of neutron damage on the critical current of several technical superconductors.

Figure 2. Torodial field ripple at the outer plasma edge vs number of coils for coils having J_{pack} = 60 A·mm^{-2} and 0.2-m build.

Figure 3. Examples to illustrate the effect of reducing J_{pack} and spreading the windings on field ripple at the outer plasma edge.

Figure 4. A typical mapping of the stability parameter Δ h in the (f_{cond}, f_{Cu}) plane. For the case displayed, B = 6.21 T, J = 68 A·mm^{-2}, T_b = 4.9 K, J_{c0} = 5200 A·mm^{-2}, and T_c = 6.53 K. The locus of optimal f_{cond} for given f_{Cu} is shown for clarity.

Figure 5. The mapping of the stability parameter for the conditions of Fig. 4 with contours of J = J_{lim} added. Curve (A) is the locus of optima from Fig. 4. Curve (B) is the contour for J = J_{lim} with undamaged copper (RRR = 100 and magneto-resistivity appropriate for 6.21 T). Curve (C) is the contour for J = J_{lim} with the same copper and field but damage of 0.2 dpa.

Figure 6. The mapping of the stability parameter for the conditions of Fig. 4 with contours of J = J_{prot} and minimum copper added. Curves (A) and (B) are again the locus of optima and J = J_{lim} with undamaged copper, respectively. Curve (C) is the minimum acceptable copper fraction, 50 %. Curve (a) is the contour for J = J_{prot} with undamaged copper. Curves (b) and (c) were calculated with copper damage of 0.005 and 0.2 dpa, respectively.

Figure 7. Variation of optimum copper fraction f_{Cu} with cable space current density J. Curves (a), (b), and (c) correspond to undamaged copper, 0.005 dpa, and 0.2 dpa, respectively.

Figure 8. Variation of optimum conductor fraction f_{cond} with cable space current density J. Curves (a), (b), and (c) correspond to undamaged copper, 0.005 dpa, and 0.2 dpa, respectively.

Figure 9. Variation of maximum obtainable stabiliy parameter Δ h with cable space current density J. Curves (a), (b), and (c) correspond to undamaged copper, 0.005 dpa, and 0.2 dpa, respectively.

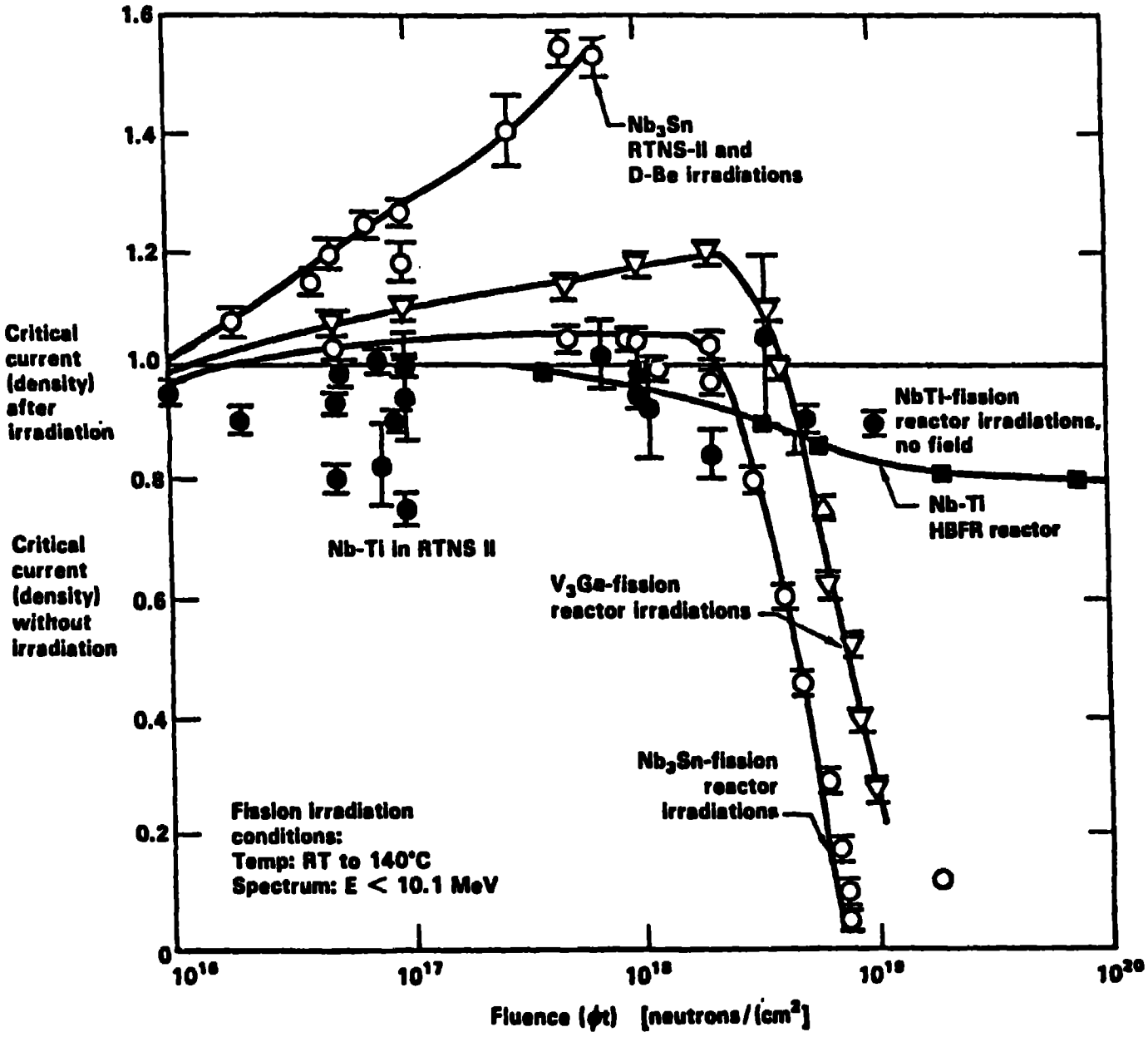
1.6
1.4
1.2
1.0
0.8
0.6
0.4
0.2
0
Critical current (density) after irradiation
Critical current (density) without irradiation
Nb3Sn RTNS-II and D-Be irradiations
NbTi-fission reactor irradiations, no field
Nb-Ti HBFR reactor
Nb-Ti in RTNS II
V3Ga-fission reactor irradiations
Nb3Sn-fission reactor irradiations
Fission irradiation conditions:
Temp: RT to 140°C
Spectrum: E < 10.1 MeV
10^16
10^17
10^18
10^19
10^20
Fluence (ϕt) [neutrons/(cm^2]

FIGURE 1

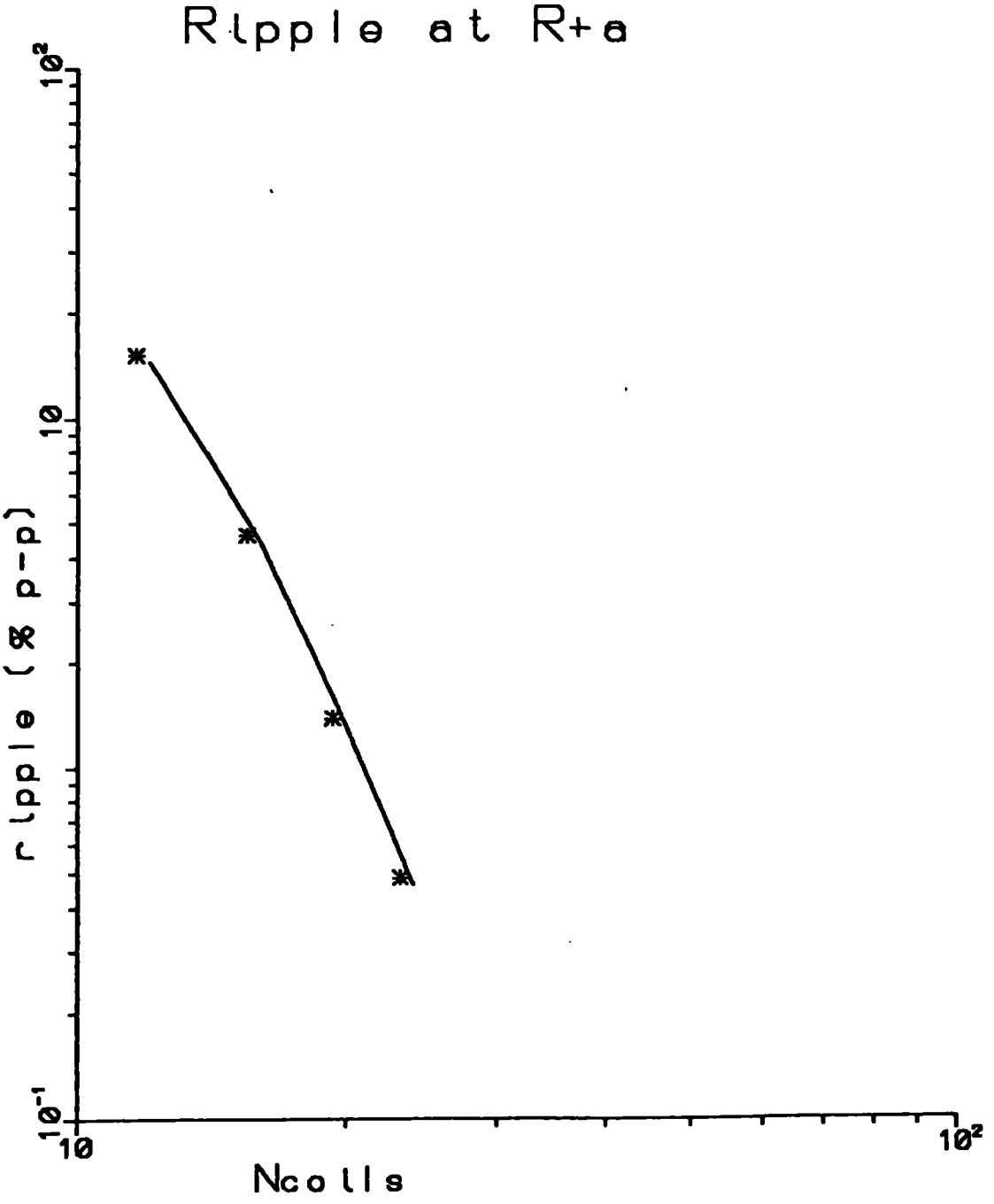

FIGURE 2

$N_{coils} = 16$

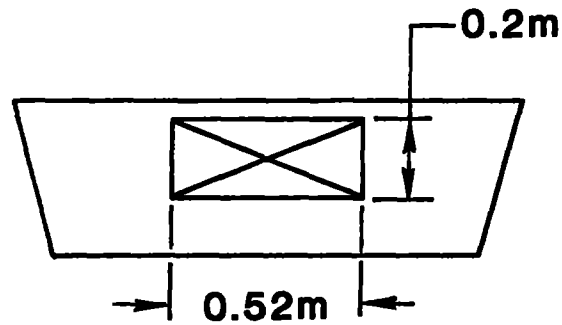

$\frac{\Delta B}{B} = 4.4\%$

at $R_o + a$

$J_{pack} = 60\ A \cdot mm^{-2}$

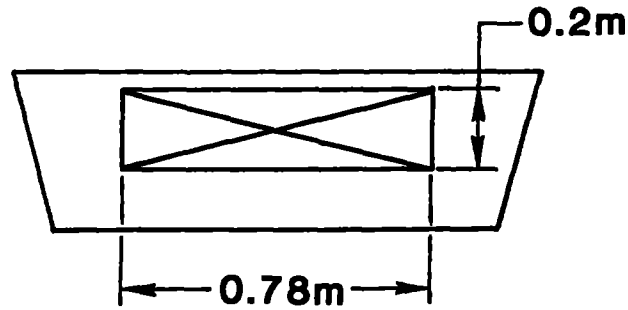

$\frac{\Delta B}{B} = 4.1\%$

$J_{pack} = 40\ A\ mm^{-2}$

FIGURE 3

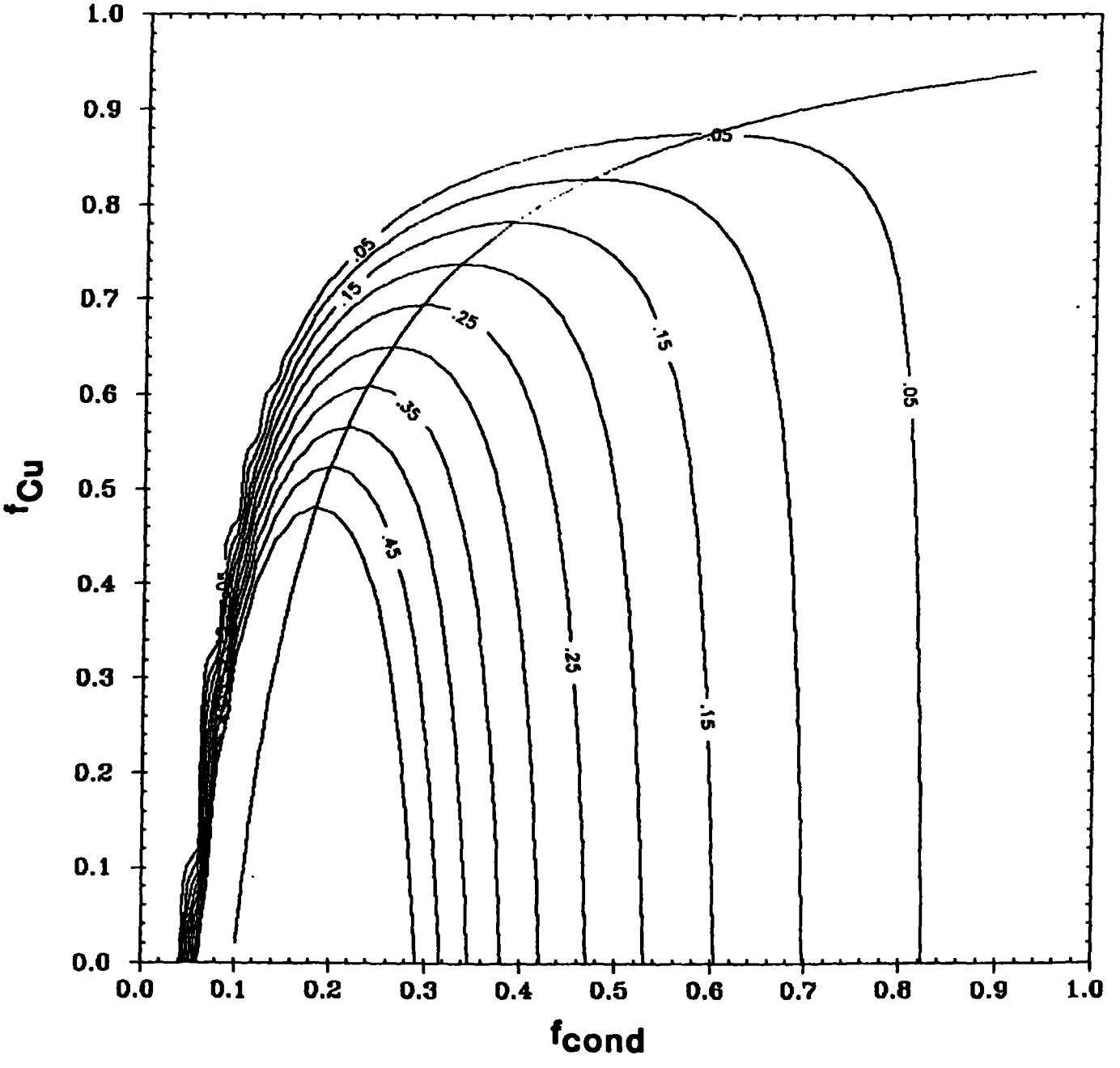
1.0
0.9
0.8
0.7
0.6
0.5
0.4
0.3
0.2
0.1
0.0
0.0
0.1
0.2
0.3
0.4
0.5
0.6
0.7
0.8
0.9
1.0
f_{Cu}
f_{cond}
.05
.15
.25
.35
.45
.05
.15
.25
.15
.05

FIGURE 4

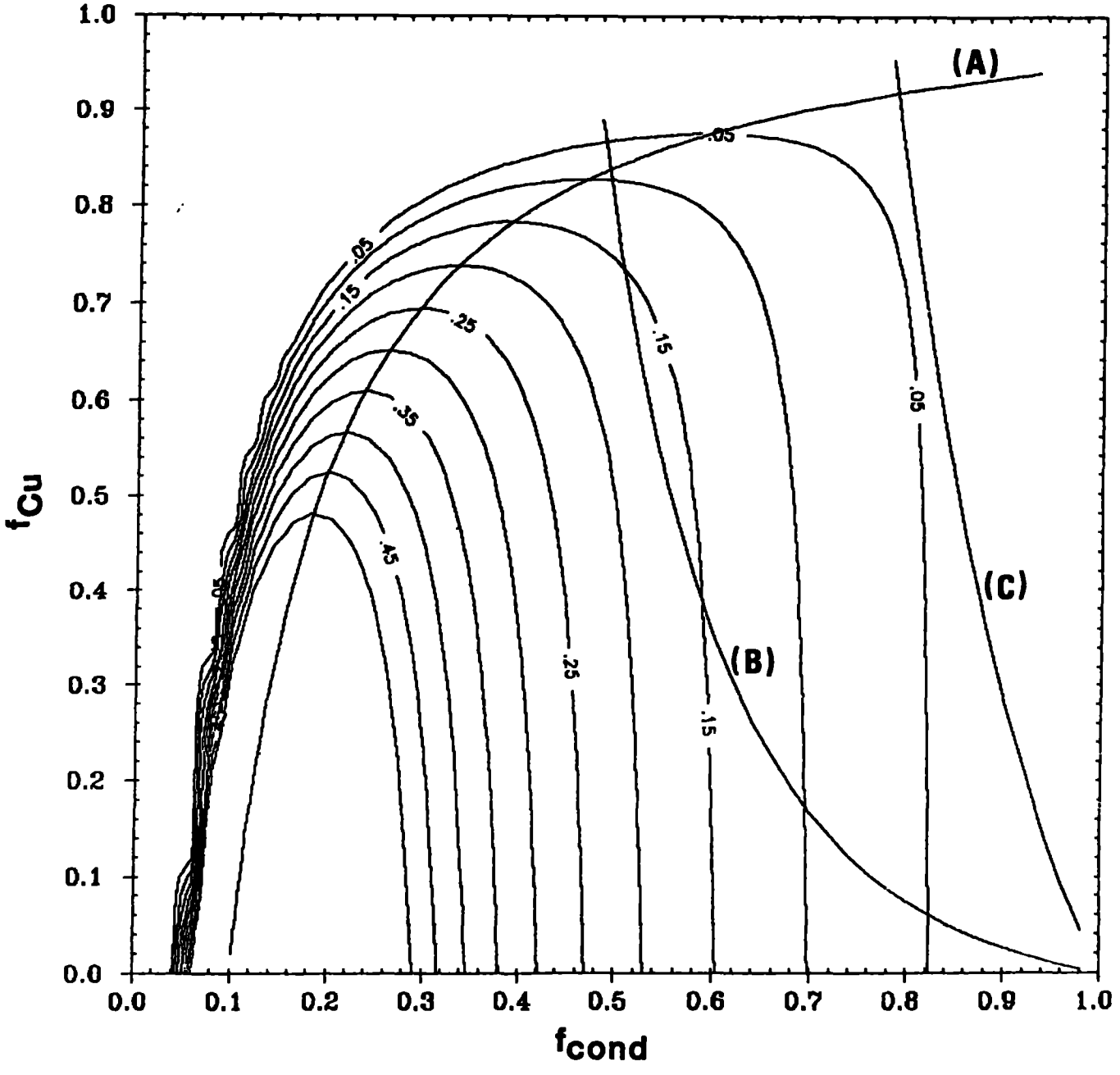
1.0
0.9
0.8
0.7
0.6
0.5
0.4
0.3
0.2
0.1
0.0
0.0
0.1
0.2
0.3
0.4
0.5
0.6
0.7
0.8
0.9
1.0
f_{Cu}
f_{cond}
(A)
(B)
(C)
.05
.15
.25
.35
.45

FIGURE 5

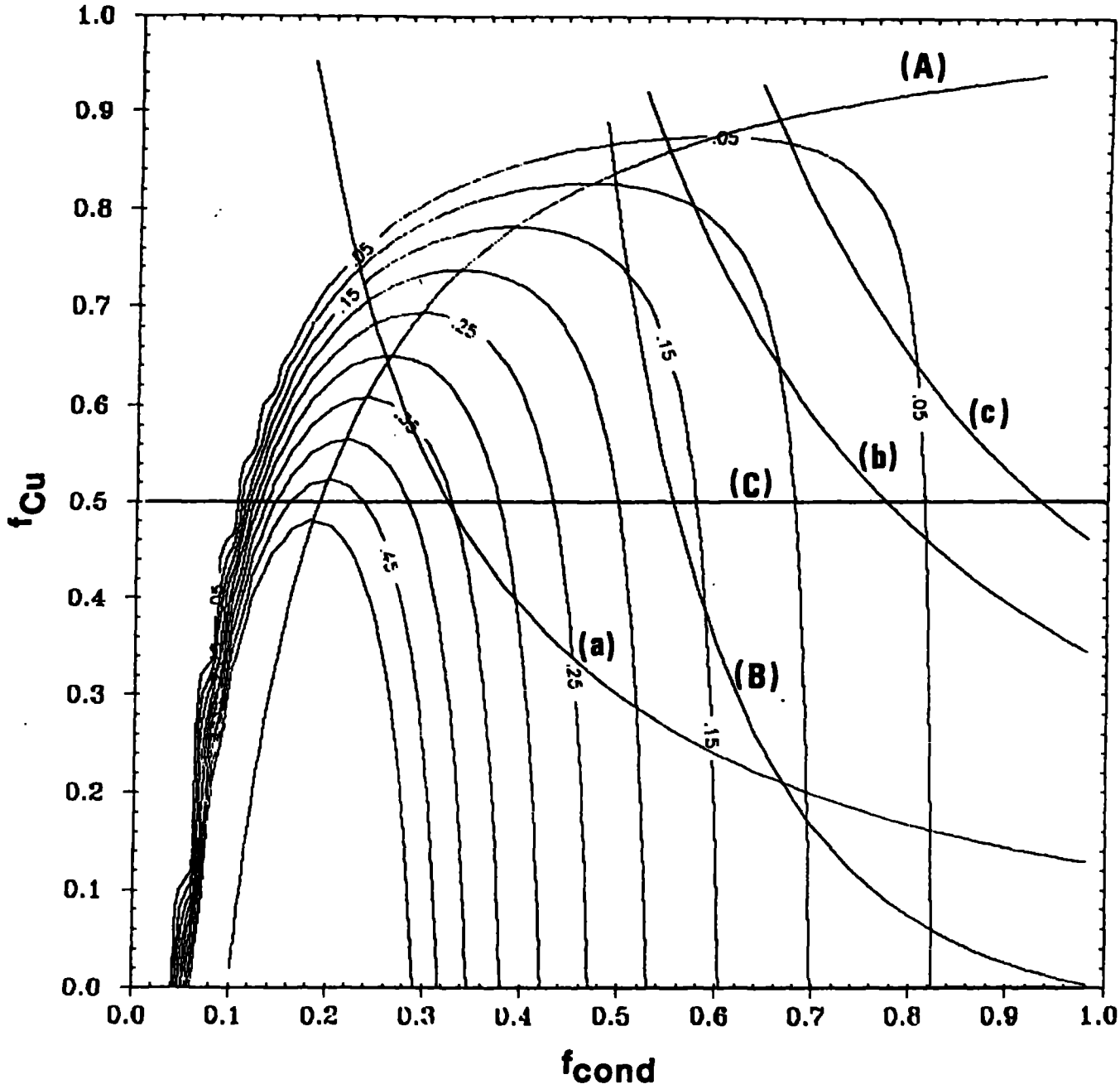
1.0
0.9
0.8
0.7
0.6
0.5
0.4
0.3
0.2
0.1
0.0
0.0
0.1
0.2
0.3
0.4
0.5
0.6
0.7
0.8
0.9
1.0
f_{Cu}
f_{cond}
(A)
(B)
(C)
(a)
(b)
(c)
.05
.15
.25
.35
.45

FIGURE 6

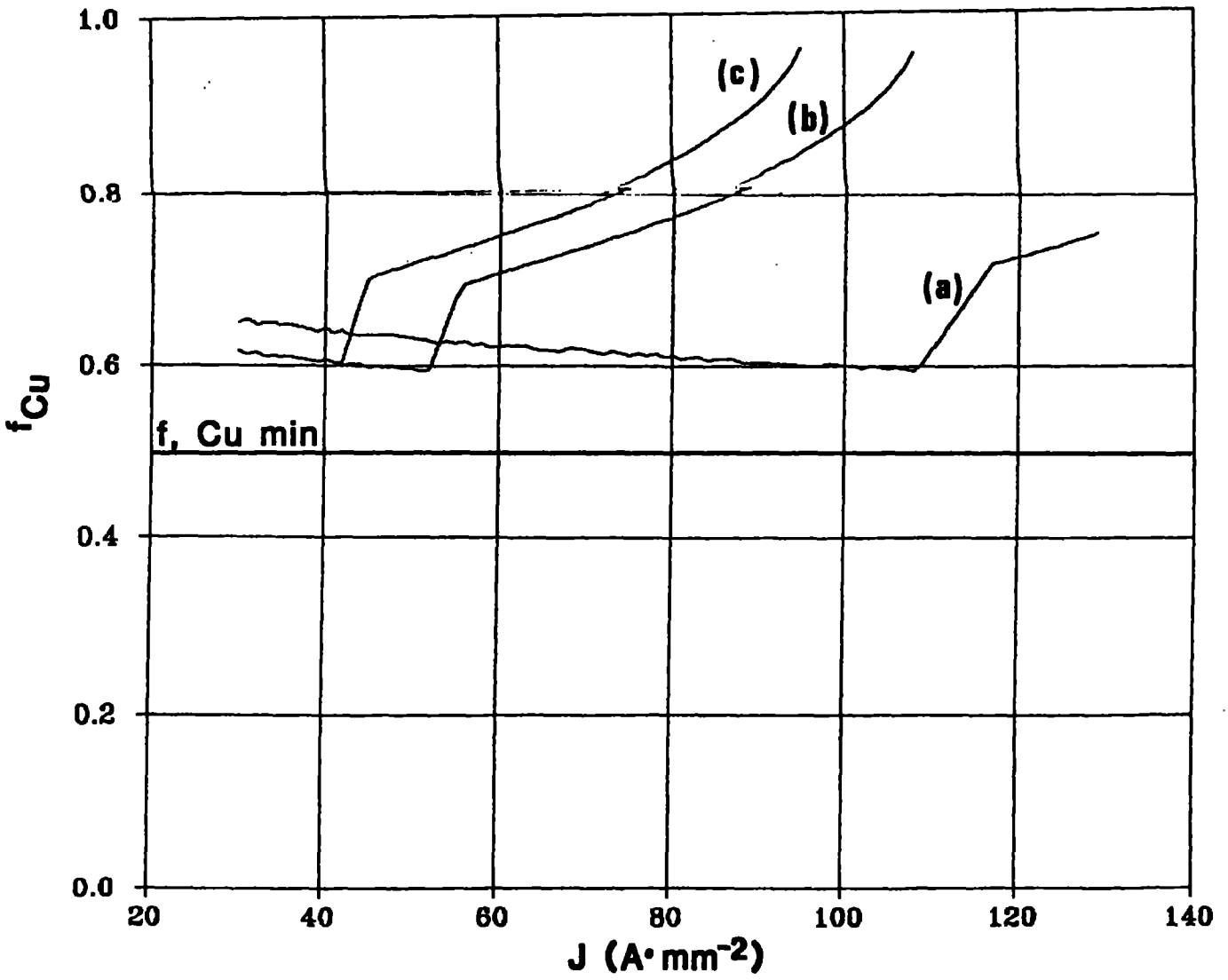

FIGURE 7

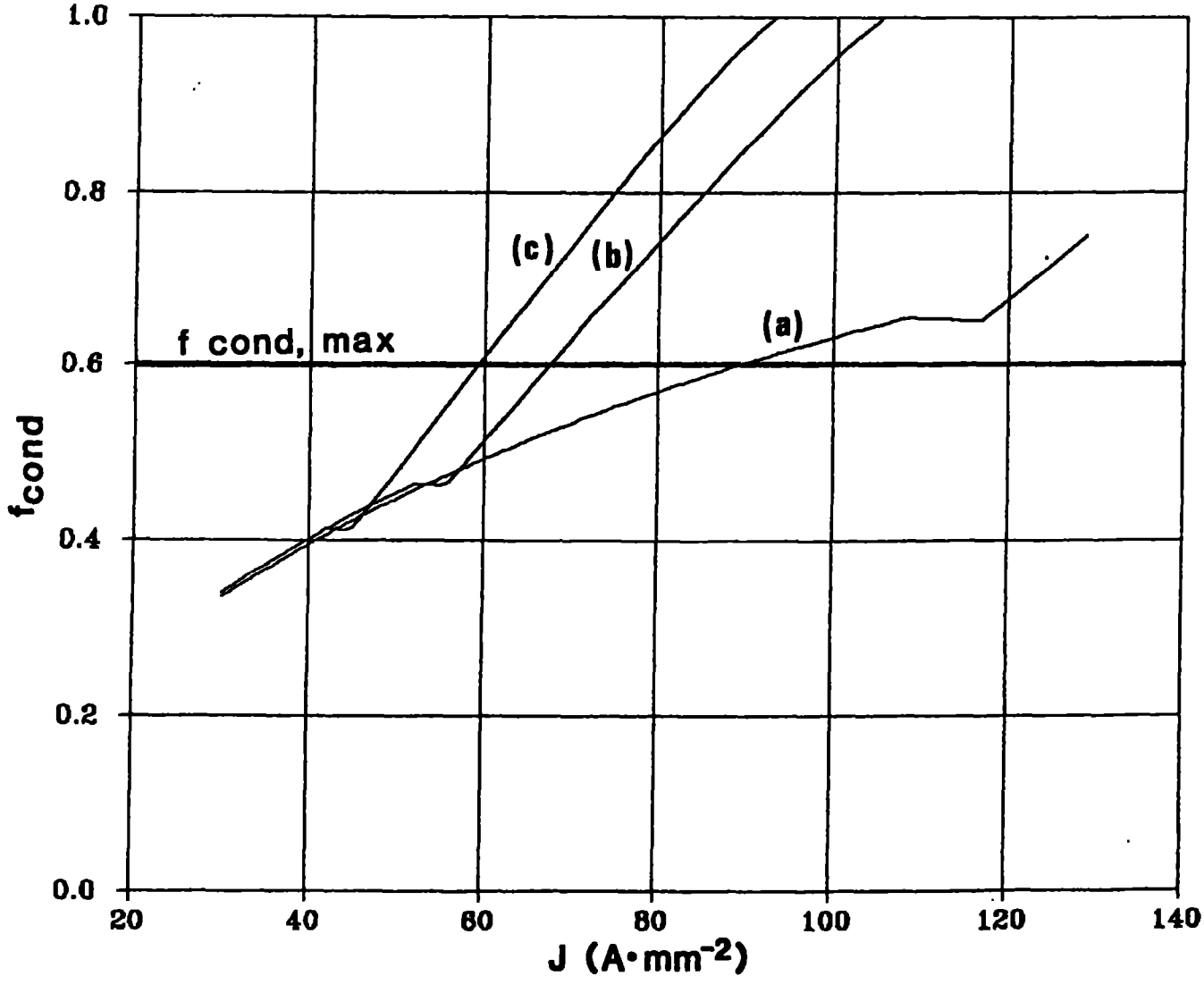
1.0
0.8
0.6
0.4
0.2
0.0
f_{cond}
f cond, max
(c)
(b)
(a)
20
40
60
80
100
120
140
J (A•mm^{-2})

FIGURE 8

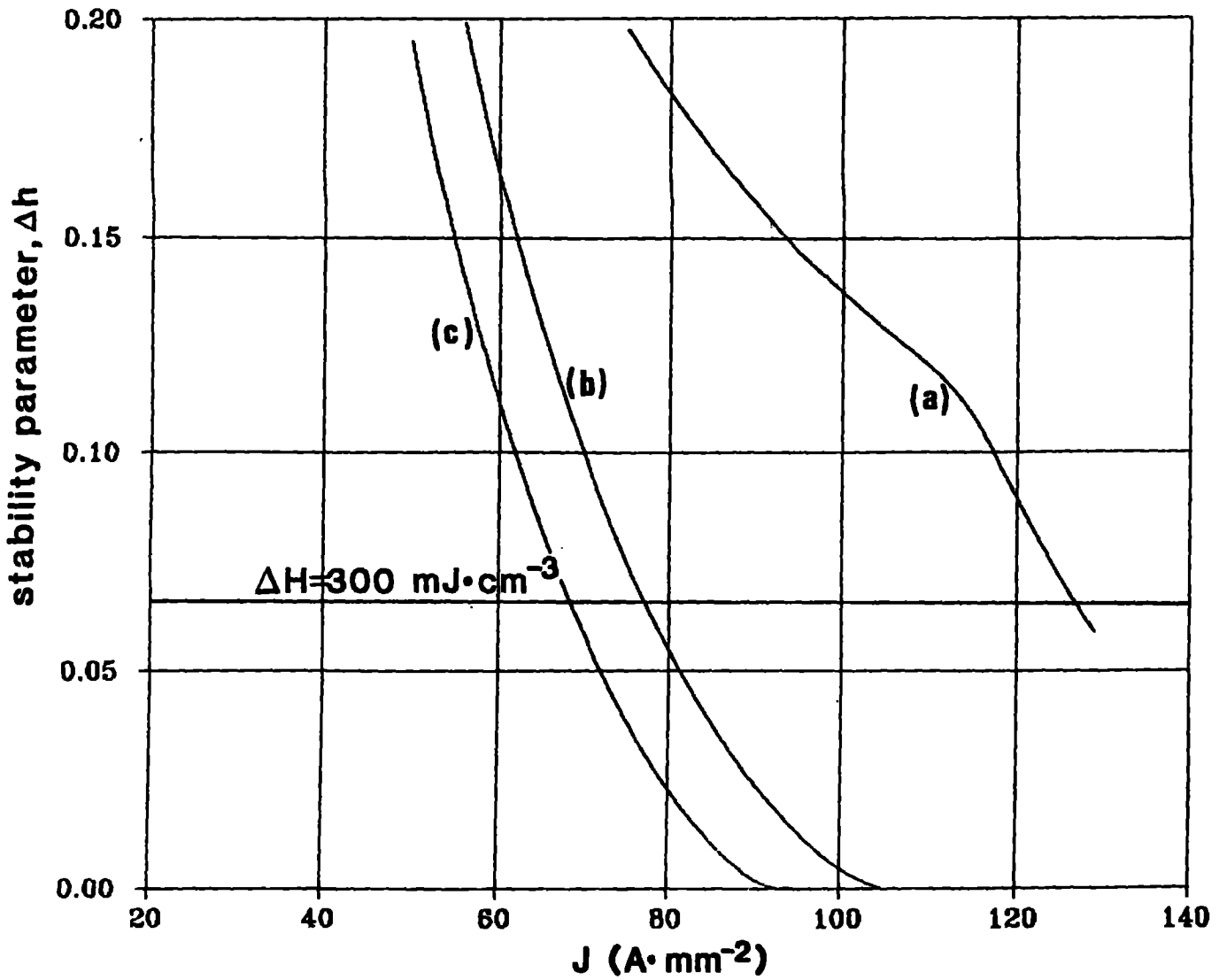
0.20
0.15
0.10
0.05
0.00
stability parameter, Δh
(c)
(b)
(a)
ΔH=300 mJ·cm⁻³
20
40
60
80
100
120
140
J (A·mm⁻²)

FIGURE 9